ROYAL SOCIETY
OF CHEMISTRY

Check for updates

Emergence of electrical conductivity in a flexible coordination polymer by using chemical reduction†

Kentaro Fuku,[a] Momoka Miyata,[a] Shinya Takaishi, [iD][a] Takefumi Yoshida, [iD][ab] Masahiro Yamashita,[abc] Norihisa Hoshino, [iD][d] Tomoyuki Akutagawa, [iD][d] Hiroyoshi Ohtsu, [iD][e] Masaki Kawano [iD][e] and Hiroaki Iguchi [iD]*[a]

A flexible coordination polymer with a naphthalenediimide core exhibited reversible desorption–adsorption of solvent molecules and an enhancement of electrical conductivity ($\sim 10^{-7}$ S cm^{-1}) upon chemical reduction using hydrazine.

Electrically conductive coordination polymers (CPs) have been one of the most attractive targets in solid-state coordination chemistry from the viewpoint of both fundamental and applied sciences.[1] For instance, Magnus-type salts,[2] and MX-[3] and MMX-type[4] chain complexes are classic but still actively investigated one-dimensional (1D) CPs owing to their conductivity,[2b,3d,e,4a,c] optical properties[3a] and potential application in nanotechnology.[4b] Recently, studies on electrically conductive CPs have been extended to 2D CPs[5] and porous CPs like so-called metal–organic frameworks (MOFs),[6] which are promising as sensors,[7] electrode materials[8] and other electronic devices.[9] In typical electrically conductive CPs, the covalent bonding character existing between metals and ligands enables carrier transport along the framework ("through-bond" conduction). On the other hand, conductive CPs with the "through-space" conduction pathway such as infinite π-stacked columns are rare.[10] Although many CPs and MOFs with large π-conjugated ligands have been reported, the ligands are mostly isolated from one another[11] or the π-stack assembly stops at the oligomer level.[12] This is because the π-stacking interaction is

generally not strong enough for compatibility with the rigid frameworks. To enhance the π-stacking interaction and to rationally design a π-stacked column among CPs, introduction of π-radicals has recently been proposed.[13,14]

In this work, we chose another strategy, that is, using flexible CPs, because flexible ligands occasionally achieve the co-existence of coordination networks and π-stacked columns.[15] A naphthalene-diimide (NDI) core was selected as the π-conjugated moiety, since it has been known as a stable electron acceptor[16] and as the main component in several conductive crystals.[17] We herein report the synthesis of a new flexible CP with the through-space conduction pathway. It showed a reversible structural change upon desorption–adsorption of chloroform molecules and an enhancement of electrical conductivity by postsynthetic carrier doping.

N,N'-Di(2-(pyridin-4yl)ethyl)-1,4,5,8-naphthalenetetracarb-oxdiimide (NDI-enpy)[18] was synthesized as the ligand, which contains flexible ethylene spacers between the NDI core and pyridyl groups. The slow diffusion of NDI-enpy in chloroform and Cu(NO$_3$)$_2$·3H$_2$O in N,N-dimethylformamide (DMF) yielded purple crystals of [Cu(NDI-enpy)$_2$(NO$_3$)$_2$]·2CHCl$_3$ (**1**). Single crystal X-ray structure analysis indicates that **1** is a 1D CP consisting of a periodic array of rectangular units, which is constructed from two NDI-enpy molecules and two Cu^{2+} ions as metal nodes (Fig. 1a). Since **1** contains a loop structure, it can be regarded as a 1D coordination network.[19] The NDI core of the ligand exhibits π–π interaction with the other NDI core in the same rectangular unit (intrachain π-stacking; red dashed lines in Fig. 1a). Although only two atom pairs are overlapped, the interatomic distance is quite short (3.175(5) Å). Moreover, the π–π interaction between NDI cores in adjacent chains (interchain π-stacking; blue dashed lines in Fig. 1a) is also formed. More atoms are involved in the interchain π–π inter-action though the interatomic distances are in the moderate range (3.228–3.477 Å). Consequently, the slipped π-stacked columnar structure is realized along the *a*-axis. As shown in Fig. 1b, the closed inner space surrounded by the NDI cores,

[a] Department of Chemistry, Graduate School of Science, Tohoku University, 6-3 Aza-Aoba, Aramaki, Sendai 980-8578, Japan. E-mail: h-iguchi@tohoku.ac.jp

[b] Advanced Institute for Materials Research, Tohoku University, 2-1-1 Katahira, Aoba-ku, Sendai 980-8577, Japan

[c] School of Materials Science and Engineering, Nankai University, Tianjin 300350, China

[d] Institute of Multidisciplinary Research for Advanced Materials, Tohoku University, 2-1-1 Katahira, Aoba-ku, Sendai 980-8577, Japan

[e] Department of Chemistry, School of Science, Tokyo Institute of Technology, 2-12-1 Ookayama, Meguro-ku, Tokyo 152-8550, Japan

† Electronic supplementary information (ESI) available: Experimental details, elemental analysis, PXRD data and a video. CCDC 1999098 (**1**). For ESI and crystallographic data in CIF or other electronic format see DOI: 10.1039/d0cc03062g
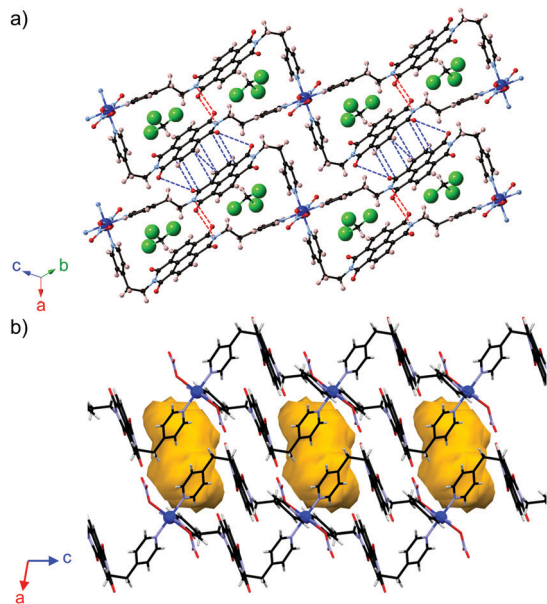
Fig. 1 Crystal structure of **1**. Each Cu ion is coordinated by four pyridyl moieties and two NO_3^- ions. (a) Short contacts (<3.5 Å) derived from $\pi-\pi$ interaction are represented as dashed lines (red: intrachain contacts, blue: interchain contacts). (b) Discrete lattice voids of approximately 12.6% of the unit cell volume are mapped by the contact surface (orange) of a probe with a radius of 1.4 Å. Two chloroform molecules exist in this closed inner space. Blue, Cu; green, Cl; black, C; light blue, N; red, O; pink or grey, H.

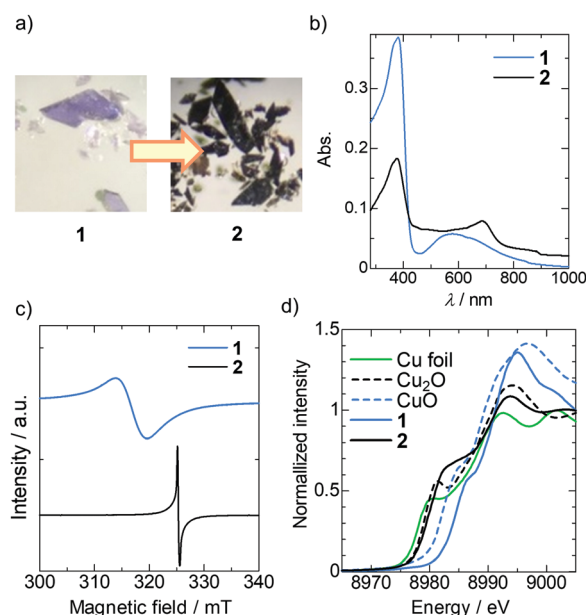pyridyl planes and NO_3^- ions (axial ligands) confines two chloroform molecules.

Thermogravimetric analysis (TGA) and differential thermal analysis (DTA) exhibited a 17.9% endothermic weight loss from 170 to 200 °C (Fig. 2a), consistent with the weight of the two chloroform molecules (17.3%). This result indicates that the elimination of chloroform occurred at an abnormally high temperature compared with the boiling point of chloroform (61 °C). This high thermal stability is probably derived from the strong confinement of the chloroform molecules in **1**. In fact, the Cl···O distances between chloroform and NDI-enpy molecules (2.842(4) Å and 2.886(5) Å) are 13.1% and 11.7% shorter than the sum of the van der Waals radii,[20] respectively. This indicates the formation of halogen bonds,[21] which should
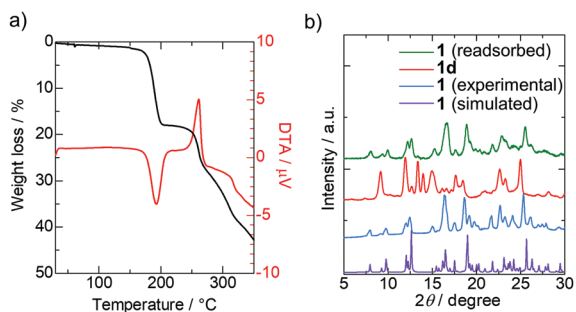
enhance the durability. The exothermic weight loss over 250 °C may indicate the decomposition of the framework. The powder X-ray diffraction (PXRD) pattern of the desolvated complex, [Cu(NDI-enpy)$_2$(NO$_3$)$_2$] (**1d**), was different from that of **1**, reflecting a large structural change of the flexible framework (Fig. 2b). The PXRD pattern, however, returned to the initial one after soaking **1d** in chloroform for a day. Thus, it is concluded that **1** is flexible enough to achieve a reversible structural change *via* desorption–adsorption of chloroform molecules.

Since **1** showed porosity and an infinite π-stacking structure, we considered postsynthetic carrier doping. To date, some NDI-based electron conductors have been reported.[17] However, the enhancement of electrical conductivity of NDI-based materials *via* electron doping has been limited to solids with dopant-accessible pores such as polymer films[22] and porous 3D MOFs,[23] to the best of our knowledge. Hence, the applicability of doping to densely packed crystalline solids has remained unclear. According to previous reports,[24] hydrazine was selected as the reductant to generate the NDI anion radical (NDI$^{\bullet-}$). In addition, it is applicable in aqueous media, where the dissolution of **1** does not occur. The postsynthetic reduction of **1** was therefore carried out by soaking **1** in an aqueous solution of hydrazine monohydrate, yielding black solid **2**, as shown in Fig. 3a. The colour change proceeded from the surface to the inside with the evolution of bubbles (see video in the ESI†), suggesting the reaction of hydrazine ($N_2H_4 \rightarrow N_2 + 4H^+ + 4e^-$). On the basis of PXRD measurement (Fig. S1, ESI†), **2** is a crystalline solid, and its crystal structure is different from that of either **1** or **1d**. The reduction of **1d** using the same method also gave a similar PXRD pattern, and thus the

Fig. 2 (a) TGA and DTA trace of **1**. (b) PXRD patterns of **1d** (red) and **1** (simulated from the crystal structure: purple, experimental: blue, after soaking **1d** in chloroform for a day: green).

Fig. 3 (a) Colour change from **1** to **2** achieved by chemical doping. (b) Solid-state UV-Vis-NIR diffuse reflectance spectra of **1** (blue) and **2** (black). (c) ESR spectra of **1** (blue) and **2** (black). (d) XANES spectra of the Cu K-edge for **1** (blue), **2** (black), Cu foil (green), Cu$_2$O (black dashed line), and CuO (blue dashed line).

structure of the reduced state **2** is not affected by the existence of chloroform molecules.

In order to study the electronic state of **2**, UV-vis-NIR diffuse reflectance spectra of **1** and **2** were acquired. As shown in Fig. 3b, the absorption band derived from the π–π^* transition in the NDI-enpy moiety was observed below 400 nm in both **1** and **2**. A relatively weak Cu^{2+} d–d absorption band was observed around 550 nm in **1**. However, this d–d band was unclear and a new peak appeared around 690 nm in the case of **2**. This new absorption band was assigned to the intramolecular transition of the $NDI^{\bullet-}$ core according to previous reports.[25] The ESR spectra exhibited a more distinct difference between **1** and **2**. As shown in Fig. 3c, a broad signal ($g = 2.0594$) attributed to the unpaired d electron of Cu^{2+} was observed in the spectrum of **1**. On the other hand, a sharp signal ($g = 2.0031$) appeared in the spectrum of **2**. Because a sharp signal is typically observed for $NDI^{\bullet-}$ species, the ESR spectra indicate that both NDI cores and Cu^{2+} ions were reduced to $NDI^{\bullet-}$ and nonmagnetic Cu^+ ions, respectively. In order to further confirm the oxidation state of the Cu atom, X-ray absorption near edge structure (XANES) spectra of the Cu K-edge were acquired at room temperature. In general, the onset of the absorption edge (E_{edge}) of a metal ion decreases with the decrease of the oxidation number. As shown in Fig. 3d, the E_{edge} of **2** was smaller than that of **1**, indicating a lower oxidation number of the Cu ion in **2**. Moreover, compared with the reference samples (Cu^0 foil, Cu^+_2O and $Cu^{2+}O$), the E_{edge} and the shape of the XANES spectra of **1** and **2** were similar to those of CuO and Cu_2O, respectively. Therefore, we conclude that the oxidation state of the Cu atom in **2** is +1.

IR spectroscopy, TGA, and elemental analysis were performed to determine the chemical formula of **2**. In the IR spectra, the signals of the C–Cl stretching vibration mode (756 cm^{-1})[26] and N–O stretching vibration mode (1388 cm^{-1})[27] disappeared after the reduction (Fig. 4a and b). These results suggest that elimination of nitrate and chloroform occurred during the reduction. Therefore, we assumed the chemical formula of the framework in **2** to be $[Cu(NDI\text{-}enpy)_2]$. From the thermogravimetric analysis of **2**, an 8.0% weight loss was observed from 30 to 260 °C (Fig. 4d). This corresponds to the elimination of five water molecules (8.1%), consistent with the results of the elemental analysis (see the ESI†). Accordingly, the chemical formula of **2** was determined as $[Cu(NDI\text{-}enpy)_2]\cdot 5H_2O$. Because the charge of the Cu ion is +1, the average charge of the NDI core is presumed to be −0.5.

The electrical conductivity (σ) of **1** and **2** was measured in pressed pellet form by using a two-probe method. The σ of **1** was below the lower detection limit of the source meter ($\sigma < 10^{-9}$ S cm^{-1}), which agrees with the lack of carriers in the π-stacked column. In contrast, **2** showed semiconducting behaviour and σ reached over 10^{-7} S cm^{-1} at room temperature, as shown in Fig. 5, reflecting the carrier doping in the π-stacked column achieved by the reduction. The activation energy (E_a) was calculated to be 0.267 eV from the Arrhenius model ($\sigma = \sigma_0 \exp(-E_a/k_B T)$), where k_B is the Boltzmann constant and T is the temperature. Although the crystal structure of **2** has not been identified, the emergence of σ strongly suggests the retention of the π-stacked columnar structure.

Fig. 4 (a–c) IR absorption spectra of **1** (blue) and **2** (black). The red dashed lines in (a) and (b) represent the reported absorption wavenumber for the C–Cl vibration mode (feature of chloroform) and N–O vibration mode (feature of NO_3^- ion), respectively. (d) TGA and DTA trace of **2**.
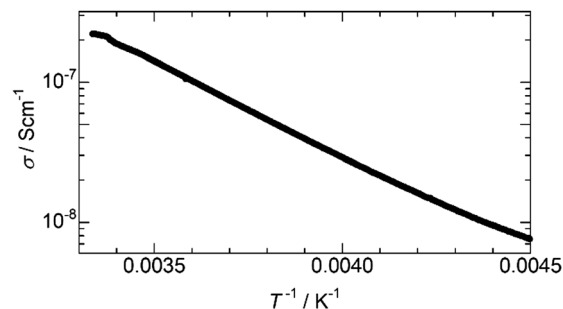

Fig. 5 Temperature dependence of the electrical conductivity (σ) of **2** measured by using a two-probe method on a pellet sample.

This is also supported by the manifestation of the broad band from 3000 to 6000 cm^{-1} (Fig. 4c), which is typically attributed to intermolecular charge transfer between NDI cores in the π-stacked column.[14]

In summary, we synthesized a flexible 1D coordination network, $[Cu(NDI\text{-}enpy)_2(NO_3)_2]\cdot 2CHCl_3$ (**1**), which shows a reversible structural change upon desorption–adsorption of internally accommodated chloroform molecules. The flexible ethylene moiety in **1** enables the co-existence of the CP framework and the infinite π-stacked column as a through-space conduction pathway. **1** demonstrated electrical conductivity upon hydrazine reduction. To the best of our knowledge, **1** is the first densely packed CP that undergoes postsynthetic carrier doping with a structural change, enabled by its flexible feature. This work offers a new basis for designing electrically conductive CPs as conductive soft crystals.[28]

Conflicts of interest

The authors declare no competing financial interest.

Notes and references

1 G. Givaja, P. Amo-Ochoa, C. J. Gómez-García and F. Zamora, *Chem. Soc. Rev.*, 2012, **41**, 115.

2 (a) E.-G. Kim, K. Schmidt, W. R. Caseri, T. Kreouzis, N. Stingelin-Stutzmann and J.-L. Brédas, *Adv. Mater.*, 2006, **18**, 2039; (b) C. H. Hendon, A. Walsh, N. Akiyama, Y. Konno, T. Kajiwara, T. Ito, H. Kitagawa and K. Sakai, *Nat. Commun.*, 2016, **7**, 11950.

3 (a) H. Kishida, H. Matsuzaki, H. Okamoto, T. Manabe, M. Yamashita, Y. Taguchi and Y. Tokura, *Nature*, 2000, **405**, 929; (b) M. Yamashita and S. Takaishi, *Chem. Commun.*, 2010, **46**, 4438; (c) S. Kumagai, S. Takaishi, H. Iguchi and M. Yamashita, *Dalton Trans.*, 2015, **44**, 8590; (d) M. R. Mian, H. Iguchi, S. Takaishi, H. Murasugi, T. Miyamoto, H. Okamoto, H. Tanaka, S. Kuroda, B. K. Breedlove and M. Yamashita, *J. Am. Chem. Soc.*, 2017, **139**, 6562; (e) M. R. Mian, U. Afrin, H. Iguchi, S. Takaishi, T. Yoshida, T. Miyamoto, H. Okamoto, H. Tanaka, S. Kuroda and M. Yamashita, *CrystEngComm*, 2020, **22**, 3999.

4 (a) M. Mitsumi, K. Kitamura, A. Morinaga, Y. Ozawa, M. Kobayashi, K. Toriumi, Y. Iso, H. Kitagawa and T. Mitani, *Angew. Chem., Int. Ed.*, 2002, **41**, 2767; (b) L. Welte, A. Calzolari, R. D. Felice, F. Zamora and J. Gómez-Herrero, *Nat. Nanotechnol.*, 2010, **5**, 110; (c) H. Iguchi, S. Takaishi and M. Yamashita, *Chem. Lett.*, 2014, **43**, 69.

5 (a) H. Miyasaka, N. Motokawa, S. Matsunaga, M. Yamashita, K. Sugimoto, T. Mori, N. Toyota and K. R. Dunbar, *J. Am. Chem. Soc.*, 2010, **132**, 1532; (b) X. Huang, P. Sheng, Z. Tu, F. Zhang, J. Wang, H. Geng, Y. Zou, C.-A. Di, Y. Yi, Y. Sun, W. Xu and D. Zhu, *Nat. Commun.*, 2015, **6**, 7408.

6 (a) S. Takaishi, M. Hosoda, T. Kajiwara, H. Miyasaka, M. Yamashita, Y. Nakanishi, Y. Kitagawa, K. Yamaguchi, A. Kobayashi and H. Kitagawa, *Inorg. Chem.*, 2009, **48**, 9048; (b) C. F. Leong, P. M. Usov and D. M. D'Alessandro, *MRS Bull.*, 2016, **41**, 858; (c) W.-H. Li, W.-H. Deng, G.-E. Wang and G. Xu, *EnergyChem*, 2020, **2**, 100029; (d) L. S. Xie, G. Skorupskii and M. Dinca, *Chem. Rev.*, 2020, DOI: 10.1021/acs.chemrev.9b00766.

7 (a) A. Chidambaram and K. C. Stylianou, *Inorg. Chem. Front.*, 2018, **5**, 979; (b) V. Rubio-Giménez, N. Almora-Barrios, G. Escorcia-Ariza, M. Galbiati, M. Sessolo, S. Tatay and C. Martí-Gastaldo, *Angew. Chem., Int. Ed.*, 2018, **57**, 15086; (c) M. L. Aubrey, M. T. Kapelewski, J. F. Melville, J. Oktawiec, D. Presti, L. Gagliardi and J. R. Long, *J. Am. Chem. Soc.*, 2019, **141**, 5005; (d) J. Chen, Y. Sekine, A. Okazawa, H. Sato, W. Kosaka and H. Miyasaka, *Chem. Sci.*, 2020, **11**, 3610.

8 (a) L. Wang, Y. Han, X. Feng, J. Zhou, P. Qi and B. Wang, *Coord. Chem. Rev.*, 2016, **307**, 361; (b) D. Sheberla, J. C. Bachman, J. S. Elias, C.-J. Sun, Y. Shao-Horn and M. Dincă, *Nat. Mater.*, 2017, **16**, 220; (c) M. E. Ziebel, C. A. Gaggioli, A. B. Turkiewicz, W. Ryu, L. Gagliardi and J. R. Long, *J. Am. Chem. Soc.*, 2020, **142**, 2653.

9 (a) D. M. D'Alessandro, *Chem. Commun.*, 2016, **52**, 8957; (b) I. Stassen, N. Burtch, A. Talin, P. Falcaro, M. Allendorf and R. Ameloot, *Chem. Soc. Rev.*, 2017, **46**, 3185.

10 (a) S. S. Park, E. R. Hontz, L. Sun, C. H. Hendon, A. Walsh, T. Van Voorhis and M. Dincă, *J. Am. Chem. Soc.*, 2015, **137**, 1774; (b) D. Chen, H. Xing, Z. Su and C. Wang, *Chem. Commun.*, 2016, **52**, 2019; (c) X. Kuang, S. Chen, L. Meng, J. Chen, X. Wu, G. Zhang, G. Zhong, T. Hu, Y. Li and C.-Z. Lu, *Chem. Commun.*, 2019, **55**, 1643.

11 (a) M. Pan, X. M. Lin, G. B. Li and C. Y. Su, *Coord. Chem. Rev.*, 2011, **255**, 1921; (b) A. Mallick, B. Garai, M. A. Addicoat, P. S. Petkov, T. Heine and R. Banerjee, *Chem. Sci.*, 2015, **6**, 1420; (c) S. Suginome, H. Sato, A. Hori, A. Mishima, Y. Harada, S. Kusaka, R. Matsuda, J. Pirillo, Y. Hijikata and T. Aida, *J. Am. Chem. Soc.*, 2019, **141**, 15649.

12 (a) S. S. Park, C. H. Hendon, A. J. Fielding, A. Walsh, M. O'Keeffe and M. Dincă, *J. Am. Chem. Soc.*, 2017, **139**, 3619; (b) C. Hua, P. W. Doheny, B. Ding, B. Chan, M. Yu, C. J. Kepert and D. M. D'Alessandro, *J. Am. Chem. Soc.*, 2018, **140**, 6622.

13 (a) J. Y. Koo, Y. Yakiyama, G. R. Lee, J. Lee, H. C. Choi, Y. Morita and M. Kawano, *J. Am. Chem. Soc.*, 2016, **138**, 1776; (b) J. Y. Ha, J. Y. Koo, H. Ohtsu, Y. Yakiyama, K. Kim, D. Hashizume and M. Kawano, *Angew. Chem., Int. Ed.*, 2018, **57**, 4717.

14 L. Qu, H. Iguchi, S. Takaishi, F. Habib, C. F. Leong, D. M. D'Alessandro, T. Yoshida, H. Abe, E. Nishibori and M. Yamashita, *J. Am. Chem. Soc.*, 2019, **141**, 6802.

15 (a) C.-L. Chen, C.-Y. Su, Y.-P. Cai, H.-X. Zhang, A.-W. Xu, B.-S. Kang and H.-C. zur Loye, *Inorg. Chem.*, 2003, **42**, 3738; (b) C. Jia, Q. Lin and W. Yuan, *CrystEngComm*, 2014, **16**, 2508.

16 M. Al Kobaisi, S. V. Bhosale, K. Latham, A. M. Raynor and S. V. Bhosale, *Chem. Rev.*, 2016, **116**, 11685.

17 (a) G. Heywang, L. Born, H.-G. Fitzky, T. Hassel, J. Hocker, H.-K. Müller, B. Pittel and S. Roth, *Angew. Chem., Int. Ed. Engl.*, 1989, **28**, 483; (b) A. Mizuno, Y. Shuku, R. Suizu, M. M. Matsushita, M. Tsuchiizu, D. R. Mañneru, F. Illas, V. Robert and K. Awaga, *J. Am. Chem. Soc.*, 2015, **137**, 7612; (c) M. T. Nguyen, M. D. Krzyaniak, M. Owczarek, D. P. Ferris, M. R. Wasielewski and J. F. Stoddart, *Angew. Chem., Int. Ed.*, 2017, **56**, 5795.

18 Y. Tsukada, K. Hirao and J. Mizuguchi, *Acta Crystallogr., Sect. E: Struct. Rep. Online*, 2007, **63**, o3872.

19 S. R. Batten, N. R. Champness, X.-M. Chen, J. Garcia-Martinez, S. Kitagawa, L. Öhrström, M. O'Keeffe, M. P. Suh and J. Reedijk, *Pure Appl. Chem.*, 2013, **85**, 1715.

20 A. Bondi, *J. Phys. Chem.*, 1964, **68**, 441.

21 G. Cavallo, P. Metrangolo, R. Milani, T. Pilati, A. Priimagi, G. Resnati and G. Terraneo, *Chem. Rev.*, 2016, **116**, 2478.

22 (a) H. Luo, Z. Liu, Z. Cai, L. Wu, G. Zhang, C. Liu and D. Zhang, *Chin. J. Chem.*, 2012, **30**, 1453; (b) Y. Han, Z. Fei, Y.-H. Lin, J. Martin, F. Tuna, T. D. Anthopoulos and M. Heeney, *npj Flexible Electron.*, 2018, **2**, 11; (c) Y. M. Gross, D. Trefz, C. Dingler, D. Bauer, V. Vijayakumar, V. Untilova, L. Biniek, M. Brinkmann and S. Ludwigs, *Chem. Mater.*, 2019, **31**, 3542.

23 (a) Z. Guo, D. K. Panda, K. Maity, D. Lindsey, T. G. Parker, T. E. Albrecht-Schmitt, J. L. Barreda-Esparza, P. Xiong, W. Zhou and S. Saha, *J. Mater. Chem. C*, 2016, **4**, 894; (b) H. Wentz, G. Skorupskii, A. B. Bonfim, J. L. Mancuso, C. H. Hendon, E. H. Oriel, G. T. Sazama and M. G. Campbell, *Chem. Sci.*, 2020, **11**, 1342.

24 D. Zhou, Y. Wang, J. Jia, W. Yu, B. Qu, X. Li and X. Sun, *Chem. Commun.*, 2015, **51**, 10656.

25 (a) D. Gosztola, M. P. Niemczyk, W. Svec, A. S. Lukas and M. R. Wasielewski, *J. Phys. Chem. A*, 2000, **104**, 6545; (b) Y. Matsunaga, K. Goto, K. Kubono, K. Sako and T. Shinmyozu, *Chem. – Eur. J.*, 2014, **20**, 7309.

26 DBS Web: https://sdbs.db.aist.go.jp National Institute of Advanced Industrial Science and Technology, accessed April 2020.

27 F. A. Miller and C. H. Wilkins, *Anal. Chem.*, 1952, **24**, 1253.

28 M. Kato, H. Ito, M. Hasegawa and K. Ishii, *Chem. – Eur. J.*, 2019, **25**, 5105.